

Right-sided dominance of the bilateral vestibular system in the upper brainstem and thalamus

Marianne Dieterich^{1,2,3,4} · V. Kirsch^{1,2,3}  · T. Brandt^{2,3,5}

Received: 11 January 2017/Revised: 6 March 2017/Accepted: 10 March 2017/Published online: 18 March 2017
© Springer-Verlag Berlin Heidelberg 2017

Abstract MRI diffusion tensor imaging tractography was performed on the bilateral vestibular brainstem pathways, which run from the vestibular nuclei via the paramedian and posterolateral thalamic subnuclei to the parieto-insular vestibular cortex. Twenty-one right-handed healthy subjects participated. Quantitative analysis revealed a rope-ladder-like system of vestibular pathways in the brainstem with crossings at pontine and mesencephalic levels. Three structural types of right–left fiber distributions could be delineated: (1) evenly distributed pathways at the lower pontine level from the vestibular nuclei to the pontine crossing, (2) a moderate, pontomesencephalic right-sided lateralization between the pontine and mesencephalic crossings, and (3) a further increase of the right-sided lateralization above the mesencephalic crossing leading to the

thalamic vestibular subnuclei. The increasing lateralization along the brainstem was the result of an asymmetric number of pontine and mesencephalic crossing fibers which was higher for left-to-right crossings. The dominance of the right vestibular meso-diencephalic circuitry in right-handers corresponds to the right-hemispheric dominance of the vestibular cortical network. The structural asymmetry apparent in the upper brainstem might be interpreted in relation to the different functions of the vestibular system depending on their anatomical level: a symmetrical sensorimotor reflex control of eye, head, and body mediated by the lower brainstem; a lateralized right-sided upper brainstem–thalamic function as part of the dominant right-sided cortical/subcortical vestibular system that enables a global percept of body motion and orientation in space.

This manuscript is part of a supplement sponsored by the German Federal Ministry of Education and Research within the funding initiative for integrated research and treatment centers.

M. Dieterich and V. Kirsch contributed equally to this work.

✉ Marianne Dieterich
marianne.dieterich@med.uni-muenchen.de

- ¹ Department of Neurology, University Hospital, Ludwig-Maximilian University Munich, Marchioninistraße 15, 81377 München, Germany
- ² Graduate School of Systemic Neuroscience, Ludwig-Maximilian University Munich, Munich, Germany
- ³ German Center for Vertigo and Balance Disorders, Ludwig-Maximilian University Munich, Munich, Germany
- ⁴ Munich Cluster for Systems Neurology (SyNergy), Munich, Germany
- ⁵ Clinical Neuroscience, Ludwig-Maximilian University Munich, Munich, Germany

Keywords DTI tractography · Vestibular system · Vestibular dominance · Brainstem · Thalamus

Introduction

The bilateral organization of human brain functions is characterized by a hemispheric specialization that is determined by phylogenetic, genetic, and developmental factors [1]. This has been primarily investigated for handedness [2] and the lateralization of language. Apparently, language does not strictly depend on handedness, since almost all right-handers and nearly 70% of left-handers have left-hemispheric control for language [3]. Hemispheric lateralization of handedness and speech is slowly established in the developing brain, appearing relatively determined by age 3 [4]. The input of sensory modalities is mediated in both hemispheres, but

lateralization may also depend on context. fMRI and MEG studies showed that the right acoustic cortex was predominantly activated during passive listening to different sound localizations [5], or when applying complex periodic sounds (in MEG [6], or during a combination of EEG and fMRI [7]).

A PET study found that the bilateral vestibular cortical network [8] has a right-hemispheric dominance in right-handers and a left-hemispheric dominance in left-handers [9]. Named study was based on caloric vestibular stimulation and could be confirmed by fMRI during galvanic vestibular stimulation [10] and auditory-evoked vestibular (otolith) stimulation [11, 12]. A meta-analytical analysis using activation likelihood estimation for the integration of then published neuroimaging results of the vestibular system found the core region of the vestibular cortical circuitry to be a parietal opercular area, OP2, and confirmed the dominance of the right hemisphere in right-handers [13]. Another meta-analysis also investigating the precise localization of the vestibular cortical network using functional MRI studies activated by caloric, galvanic, or auditory vestibular stimulation identified the retroinsular cortex (Ri), parietal operculum (OP2), and the posterior insula as core regions [14]. The latter includes the parieto-insular vestibular cortex (PIVC), which was first discovered in electrophysiological studies of the monkey [15]. The human homologue of the PIVC was first described in patients with acute circumscribed middle cerebral artery strokes [16]. Recent neurophysiological studies modulating the activity of the visual cortex V1 [17] or posterior parietal cortex (PPC) areas [18] by means of transcranial magnetic or direct current stimulation revealed a lateralized top-down influence of the visuo-vestibular network on brainstem functions such as the suppression of vestibular nystagmus.

In our initial PET study [9] we both found a global cortical hemispheric dominance and could differentiate two further determinants of lateralization. First, there was a stronger activation in the hemisphere ipsilateral to the irrigated ear (right or left ear), and second, irrigations of the right ear (in right-handers) evoked stronger activations in general than those of the left ear [19]. This raised the question whether the bilateral vestibular brainstem circuitry with its ascending fibers from the vestibular nuclei to the vestibular thalamic subnuclei is also structurally organized asymmetrically, i.e., is there a dominant side of the vestibular pathways? Such a structural asymmetry would concur with the above-described PET data. In the main ascending vestibular brainstem fibers provide a “rope-ladder” system with crossing and non-crossing fibers [20]. These fibers travel through posterolateral or paramedian thalamic regions [21, 22], and are projected from there onto the bilateral central vestibular network [8]. Three right–left

brainstem crossings connect first the vestibular nuclei at the pontomedullary level (commissural fibers), second, cross in the pons between the medial longitudinal fascicles, and third, cross at the midbrain tegmental level to connect the right and left portions of the oculomotor nuclei/interstitial nucleus of Cajal complex. It is hypothesized that the sensorimotor functions of the lower brainstem (including the vestibulo-ocular and vestibulo-spinal reflexes) do not require structural or functional lateralization, whereas the upper brainstem and thalamic system which link vestibular input to multisensory, higher vestibular functions might be incorporated into the right-sided lateralized hemispheric cortical system.

The aim of this study was to attempt a first quantification of vestibular brainstem pathways using diffusion tensor imaging (DTI) tractography. The analyses focused on both (1) the ipsi- or contralateral pathways from the vestibular nucleus to the thalamus detected in a recent study in humans using structural and functional connectivity mapping [20] and (2) the posterolateral and paramedian thalamic regions associated with vestibular dysfunction identified earlier in thalamic infarctions [21]. This technique allowed us to determine if a structural right–left asymmetry in right-handed healthy subjects forms the basis of the described functional dominance [23] in the vestibular system.

Materials and methods

Subjects

Twenty-one right-handed (RH) healthy volunteers (10 females; aged 20–47 years, mean age 27.6 ± 6.1 years) participated in the study. The laterality quotient for right-handedness according to the 10-item inventory of the Edinburgh test [24] resulted in +100% in 19, +90% in one, and +80% in the remaining one subject. Institutional Review Board (IRB) approval was obtained prior to beginning the study (project-nr: 094-10). Participants provided their informed oral and written consent in accordance with the Declaration of Helsinki.

Measurement of the semicircular canal and otolith functions

The integrity of vestibular function was ascertained by assessing the semicircular canal function with the vestibulo-ocular reflex (VOR) and the otolith function by determining the subjective visual vertical (SVV). A median gain during video-head impulses <0.8 (eye velocity in $^{\circ}/s$ divided by head velocity in $^{\circ}/s$) was considered the criterion for a pathological VOR [25]. A mean deviation of

$>2.5^\circ$ from the true vertical was considered a pathological tilt of the SVV. None of the participants showed deficits of the VOR or pathological tilts of the SVV [26].

MRI data acquisition

MR imaging data were acquired in a whole-body 3.0 Tesla MR scanner (Magnetom Verio, Siemens Healthcare, Erlangen, Germany) with a 32-channel head coil. Diffusivity was measured in 32 directions with $2.0 \times 2.0 \times 2.0 \text{ mm}^3$ isotropic voxels (TE = 110 ms, TR = 8900 ms, b values = 0 and 1000 s/mm^2). Anatomical images included a T1-weighted magnetization-prepared rapid gradient echo (MP-RAGE) sequence with a field-of-view of 256 mm and an isotropic spatial resolution of $1.0 \times 1.0 \times 1.0 \text{ mm}^3$ (TE 4.37 ms, TR = 2100 ms, number of slices 160).

Regions of interest (ROIs)

The major focus of our study was to quantify known vestibular brainstem pathways that deliver input to the parieto-insular vestibular cortex (PIVC) via different thalamic regions. These thalamic regions (Fig. 1a) were

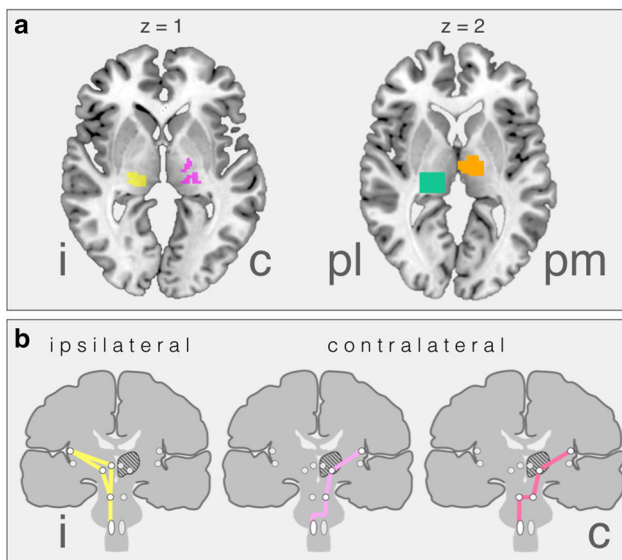


Fig. 1 To quantify known vestibular brainstem pathways that deliver input to the parieto-insular vestibular cortex (PIVC) via different thalamic regions these thalamic regions were extracted from previous studies [20, 21] and grouped differentially by laterality (ipsilateral vs. contralateral; **a left**) or topography (posterolateral, pl vs. paramedian, pm) (**a right**). Vestibular nuclei seed ROIs, brainstem waypoint ROIs (subdivided into *right* or *left* pons or midbrain ROIs), and PIVC target ROIs were created as described previously [20]. This resulted in a set consisting of one ipsilateral non-crossing pathway (**b left**) and two contralateral crossing pathways at the pons (**b middle**) or midbrain (**b right**) levels per thalamic region. **a** Depiction of the ipsilateral (*i*, yellow), contralateral (*c*, pink), posterolateral (*green*), and paramedian (*orange*) vestibular thalamus ROIs. **b** Schematic overview of the resulting vestibular pathways within the brainstem per thalamic ROI

extracted from previous studies [20, 21] and grouped differentially by laterality (ipsilateral vs. contralateral) or topography (posterolateral vs. paramedian). Vestibular nuclei seed ROIs, brainstem waypoint ROIs (subdivided into right or left pons or midbrain ROIs), and PIVC target ROIs were created as described elsewhere [20]. This yielded a threefold pathway set consisting of one non-crossing pathway and two crossing pathways (at the pons or midbrain levels) per thalamic region (Fig. 1b).

DTI preprocessing and analysis

The data were preprocessed and analyzed with FMRIB's Diffusion Toolbox as part of the FSL package (FSL v5.0.9, FDT v2.0, Oxford, UK). First, eddy current correction [27] and brain extraction [28] were applied. DTIFIT 1st eigenvector was used to check for data quality. Then the local probability density function of a diffusion tensor model was calculated using an algorithm that models intravoxel crossing fibers [29]. Structural connectivity of the brainstem to the core region of the PIVC was determined using the connectivity-based seed classification option of the FSL probabilistic tractography software: number of samples = 5000/voxel; curvature threshold = 0.2; number of steps = 2000; step length = 0.5 mm [30]. Probabilistic tracts were quantified using waytotal (w), which corresponds to the total number of generated tracts from each seed mask that reached the target mask and were not rejected by inclusion or exclusion mask criteria, and then corrected for differing ROI target size before comparing the streamline quantifications.

Statistics and map display

Statistics were performed in FSL and with the IBM SPSS Statistics software package (version 20). A participant was considered to have structural connections from the vestibular nuclei to the core region of the PIVC if any voxel in the vestibular nuclei passed a threshold of 1500 of 5000 (30%) samples or higher sent to the PIVC ROI [31]. Statistical maps were thresholded accordingly with the min (30%) and max intensity (100%). After correction for multiple testing, $p < 0.001$ was set to 0.00005. DTI maps were projected onto high-resolution T1-weighted default anatomical brain images distributed with Chris Rorden's MRIcron.

Results

In this study a right-sided (R) pathway means a pathway that reaches the right PIVC. A left-sided (L) pathway means a pathway that reaches the left PIVC. The source of

the pathway may be the left or right vestibular nuclear complex (VN), depending on an existing crossing or not. Ipsilateral (i) means no crossing and contralateral (c) means crossing on the level of the pons (p) or midbrain (m). The thalamus can be referred to as posterolateral (pl) or paramedian (pm), depending on the used waypoint ROI (region of interest).

Ipsilateral (i) vs. contralateral (c) thalamic informed brainstem pathways

The ipsilateral pathways (R_i : $w = 73,499.7 \pm 31,386.0$; L_i : $w = 72,520.4 \pm 20,284.7$) had significantly more tracts when compared to the contralateral pathways crossing in the pons (R_{cp} : $w = 2908.4 \pm 3182.9$; L_{cp} : $w = 634.3 \pm 590.9$) or mesencephalon (R_{cm} : $w = 3464.3 \pm 3126.6$; L_{cm} : $w = 1149.2 \pm 727.4$) (Table 1). Whereas the number of right (R_i)- and left (L_i)-sided ipsilateral tracts were similar, both the number of R contralateral tracts (R_{cp} ; R_{cm}) were significantly higher when compared to L (L_{cp} ; L_{cm}), and contralateral tracts crossing in the mesencephalon (L_{cm} ; R_{cm}) were significantly higher when compared to the contralateral tracts crossing in the pons (L_{cp} ; R_{cp}). Overall more streamlines reached the right PIVC ($w = 79,872.4$) when compared to the left (74,303.9). For visualization, please see Fig. 2.

Posterolateral (pl) vs. paramedian (pm) thalamic informed brainstem pathways

The ipsilateral (i), right-sided (R) pathways through the posterolateral (pl) part of the thalamus (R_{i-pl} : $w = 71,105.0 \pm 30,969.7$; L_{i-pl} : $w = 40,063.6 \pm 540.4$) and through the paramedian (pm) part of the thalamus (R_{i-pm} : $w = 63,975.9 \pm 36,299.2$; L_{i-pm} : $w = 38,369.9 \pm 20,055.8$) again had significantly more tracts when compared to the contralateral (c), left-sided (L) pathways that crossed in the pons (p; R_{cp-pl} : $w = 1459.1 \pm 1824.1$; L_{cp-pl} : $w = 611.0 \pm 580.6$; R_{cp-pm} : $w = 499.6 \pm 1014.5$; L_{cp-pm} : $w = 332.5 \pm 308.$) or mesencephalon (m; R_{cm-pl} : $w = 1717.6 \pm 1938.6$; L_{cm-pl} : $w = 921.1 \pm 642.7$; R_{cm-pm} : $w = 1578.6 \pm 1253.5$; L_{cm-pm} : $w = 1797.5 \pm 1471.2$) (Table 1). Here the number of $R_{i-pl/pm}$ was significantly higher when compared to $L_{i-pl/pm}$, the number of R contralateral tracts ($R_{cp-pl/pm}$; $R_{cm-pl/pm}$) was significantly higher when compared to L tracts ($L_{cp-pl/pm}$; $L_{cm-pl/pm}$). The number of contralateral tracts crossing in the mesencephalon ($R_{cm-pl/pm}$; $L_{cm-pl/pm}$) was significantly higher when compared to the contralateral tracts crossing in the pons ($R_{cp-pl/pm}$; $L_{cp-pl/pm}$). Overall more streamlines reached the right PIVC ($w = 140,335.8$) when compared to the left (82,095.6), and more streamlines reached the PIVC on both sides via pl ($w_R = 74,281.7$;

Table 1 Overview of DTI tractographies

	L _{waytotal}	R _{waytotal}
VT		
i	73,499.7 ± 31,386.0	72,520.4 ± 20,284.7
c _m	1149.2 ± 727.4	3464.3 ± 3126.6
c _p	634.3 ± 590.9	2908.4 ± 3182.9
i + c _m + c _p	74,303.9	79,872.4
pl		
i	40,063.6 ± 540.4	71,105.0 ± 30,969.7
c _m	921.1 ± 642.7	1717.6 ± 1938.6
c _p	611.0 ± 580.6	1459.1 ± 1824.1
i + c _m + c _p	41,595.7	74,281.7
pm		
i	38,369.9 ± 20,055.8	63,975.9 ± 36,299.2
c _m	1797.5 ± 1471.2	1578.6 ± 1253.5
c _p	332.5 ± 308	499.6 ± 1014.5
i + c _m + c _p	40,499.9	66,054.1

The analyses focused on both the ipsi (i)- or contralateral (c) pathways from the vestibular nucleus to the thalamus detected in a recent study in humans using structural and functional connectivity mapping [20] and the posterolateral (pl) and paramedian (pm) thalamic regions associated with vestibular dysfunction identified earlier in thalamic infarctions [21]. Quantification of DTI tractographies were based on “waytotal” streamlines found in the respective pathway. Waytotal corresponded to the total number of generated tracts from each seed mask (vestibular nuclei) that reached the target mask (PIVC; parieto-insular vestibular cortex) through the different vestibular informed thalamic waypoint masks. In this context, a right-sided (R) pathway means a pathway that reaches the right PIVC. A left-sided (L) pathway means a pathway that reaches the left PIVC. Note that overall more streamlines reached the right PIVC when compared to the left PIVC, independent of the thalamic region used. Further, ipsilateral pathways dominated over contralateral pathways, mesencephalic crossings over pontine crossings, and pl over pm

($w_L = 41,595.7$) when compared to pm ($w_R = 66,054.1$; $w_L = 40,499.9$).

Discussion

DTI tractography of the vestibular pathways between the pontomedullary vestibular nuclei and the paramedian (pm) and posterolateral (pl) vestibular subnuclei of the thalamus confirmed that a bilateral vestibular network with crossings in the pons and mesencephalon forms a “rope-ladder” structure. This rope-ladder system shows the following quantifiable characteristics: (1) the importance of ipsilateral non-crossing pathways (Fig. 3a), (2) the quantifiable superiority of pathways leading to the non-dominant right hemisphere (Fig. 3a, b) for both thalamic projections pl or pm (Fig. 3b), and (3) an overhang of contralateral fibers crossing in the mesencephalon when compared to the pons (Fig. 3a, b).

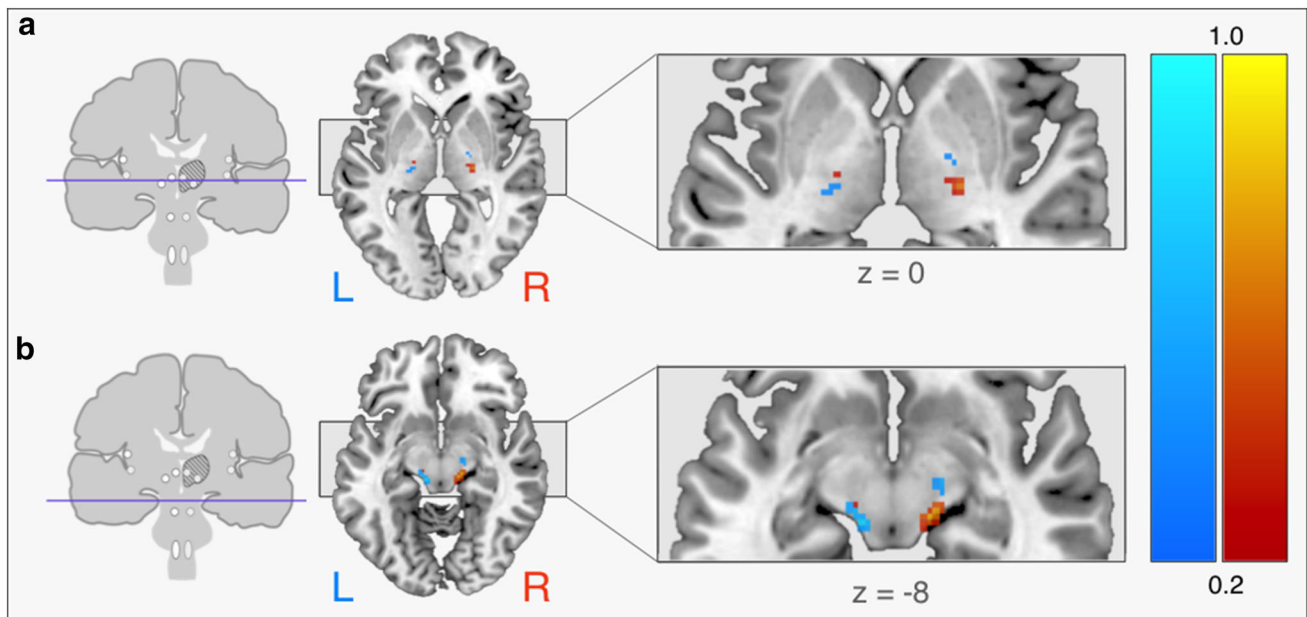


Fig. 2 Visualization of the major findings of the DTI tractographies of **a** the thalamus ($z = 0$) and **b** the upper midbrain just before arrival at the different thalamic ROIs ($z = -8$). The level is also shown as a blue line on a schematic brain map (left). DTI maps were thresholded to 0.2–1.0 of the maximally calculated probability value. All tracts

(ipsilateral and contralateral) were colored blue (left) or red (right) according to the vestibular nuclei from which they were seeded. Note the dominance of fiber tracts of the right side at midbrain and thalamic level

The structural asymmetry of the vestibular brainstem network can be cautiously quantified in terms of DTI streamlines that reached the parieto-insular vestibular cortex (PIVC) from the vestibular nuclei (VN) through specific regions of the thalamus. Asymmetry appears to increase from the lower to the upper brainstem as a consequence of the asymmetric crossings with in the whole more fibers crossing from left VN to right PIVC. This means that three levels of structural lateralization can be topographically delineated within the bilateral vestibular network in the brainstem up to the thalamus:

1. a symmetrical, lower pontine level that includes the vestibular nuclei and ipsilateral pathways up to the pontine crossing,
2. a moderate right-sided lateralization at the pontomesencephalic level between the pontine and mesencephalic fiber crossings, and
3. a further increase in right-sided lateralization above the mesencephalic crossing for pathways running to the thalamus, the vestibular subnuclei of which carry on the lateralization (Figs. 2a, 3).

The data allow us to roughly estimate the right–left relationship in terms of total streamlines arriving in the target region PIVC via distinct thalamus waypoint regions (see Fig. 3). These findings are in line with the subdivision of sensorimotor vestibular function into (a) reflexive control of gaze, head, and body in three spatial planes (yaw,

pitch, roll) at the brainstem/cerebellar level; (b) perception of self-motion and control of voluntary movement and balance at the cortical/subcortical level; (c) higher vestibular cognitive functions such as orientation, attention, spatial memory and navigation at multisensory cortical level [32].

Reflexive control, e.g., of the eyes by the VOR for maintaining gaze on target during head rotation, is based on information of head angular velocity in degrees per second. This function is probably symmetrical. Awareness of the change of head direction in space requires integration of the angular velocity signal to a head position signal. These changes in heading direction, attention, and orientation most likely involve the dominant vestibular cortical network.

The perception of angular head velocity and head direction is mediated by specialized neuronal systems that encode different features including head rotation by the angular head velocity cells and heading direction by the head direction cells [33–35]. These cells interact with hippocampal place cells and entorhinal cortex grid cells. The neuronal assemblies of angular head velocity cells which sense semicircular canal function and head direction cells have a separate but overlapping infratentorial distribution [36]. The angular head velocity cell system is especially localized in the lower brainstem, whereas the head direction cell system is mainly distributed in the upper midbrain and anterior dorsal thalamus. This explains why

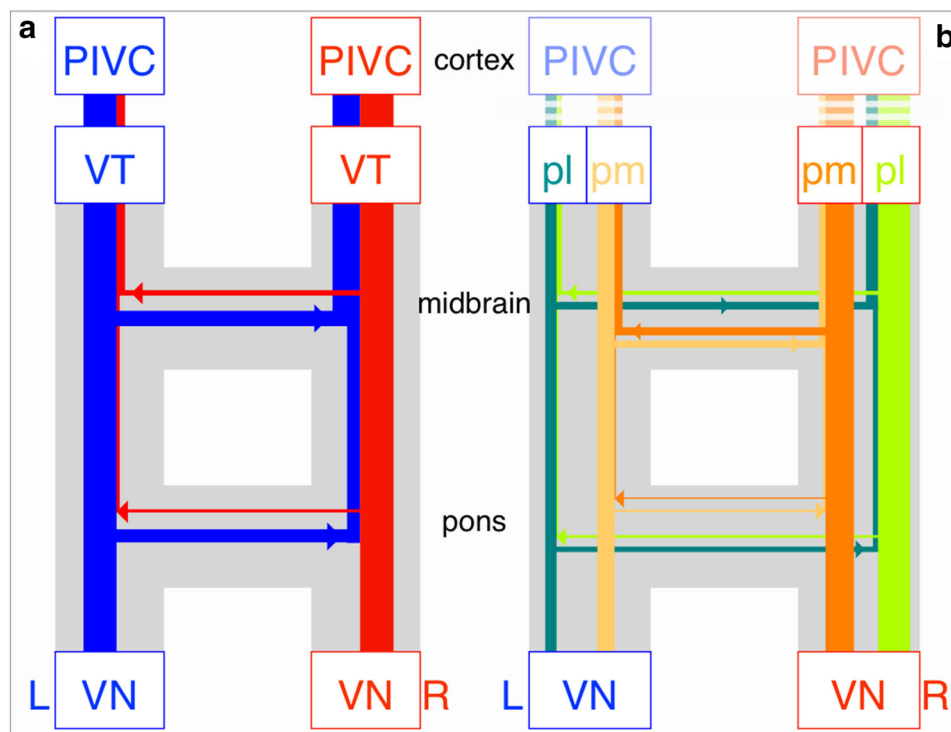


Fig. 3 Quantitative visualization of the ipsilateral (*vertical*) and contralateral (*crossing horizontally*) vestibular brainstem pathways that were informed by distinct thalamic waypoint regions of interest (ROI). Fibers cross at pontine or mesencephalic level. Thickness of the lines reflects the “waytotal” streamlines found in the respective pathway, and corresponds to the total number of generated tracts from each seed mask (vestibular nuclei; VN) that reached the target mask (PIVC; parieto-insular vestibular cortex) through the different vestibular informed thalamic waypoint masks (vestibular thalamus; VT). For quantitative details see Table 1. The direction of the *arrows* indicates the directionality of analyses from seed to target, and does not characterize the directionality of possible pathways (no distinction between afferent and efferent pathways). **a** Pathways coming from the

right (R) vestibular nucleus (VN) are colored in *red* and pathways coming from the left VN are colored in *blue*. Note that due to the asymmetrically crossing fibers in sum more streamlines arrive in the right PIVC when compared to the left. **b** Here the VT is not only divided by ipsilateral and contralateral fibers, but also into fibers passing the posterolateral (pl) or paramedian (pm) part of the thalamus. PIVC and corresponding arriving pathways were dimmed to indicate that the specific anatomical waypoints in between pm and/or pl thalamus remain as yet unclear. Please note, the overall preponderance of ipsilateral pathways over contralateral pathways, mesencephalic crossings over pontine crossings, and pathways arriving in the right PIVC over pathways arriving in the left PIVC

unilateral lower brainstem lesions manifest with rotational vertigo, whereas unilateral lesions in and above the midbrain do not [32, 37]. Thus, the distribution and function of these two vestibular cell systems may help us to understand the increasing lateralization of vestibular structures and their functions along the brainstem. The perceptual transformation of head velocity into the perception of head direction is a precondition for updating our awareness of body localization and orientation in space during locomotion. The brainstem asymmetry of the vestibular system contributes to the predominant right-hemispheric cognitive functions of orientation, spatial memory, and navigation. This view does not diminish the importance of the inter-hemispheric collaboration of the two visual–vestibular cortical networks via their transcallosal interconnections for a global percept of self-motion and orientation.

There are several methodological shortcomings in this study. The main one pertains to DTI tractography itself

[38]. DTI is characterized by a low resolution ($2.0 \times 2.0 \times 2.0 \text{ mm}^3$), limited quality (it is not possible to make a statement about excitatory or inhibitory processes), unclear directionality (inability to distinguish between afferent and efferent pathways), and a questionable accuracy when distinguishing crossing from bending fibers close to midline (this is a considerable problem). To minimize the latter problem we performed additional DTI tractography analyses focusing on crossing brainstem fibers. However, our analyses were based on known brainstem crossings. More level of crossings is possible. It is overall probable that our analyses underestimate the number of crossing fibers and overestimates the number of non-crossing fibers. In addition, a number of problems associated with quantification of the fibers based on streamlines tractograms (regardless if count or density) are known, which means that the validity of any conclusions drawn from this approach regarding brain network

properties remain uncertain and must be interpreted cautiously [39]. Another methodical limitation lies within our ROIs. It is important to note that our analyses only apply to one specific PIVC node. Add-ons in future in vivo approaches might be the use of a higher resolution of voxels, directions, and nodes within a DTI tractography. Multimodal approaches adding functional modalities and brain stimulation to this structural approach could help specify the directionality of the aforementioned pathways. Postmortem approaches such as 3D imaging of cleared human brains or high-field and high-resolution MRI imaging of the brain in combination with different tracers might be interesting tools to visualize the vestibular neuronal structural network more correctly and in its entirety. Finely, it is still an open question whether left-handers also show a dominance of the left-sided vestibular meso-diencephalic fibers as has been demonstrated for vestibular cortex structures [9].

Acknowledgements Partially funded by the Society for the Advancement of Science and Research at the Medical Faculty of the Ludwig-Maximilians-University Munich, the Graduate School of Systemic Neurosciences (GSN), the German Foundation for Neurology (DSN), the German Federal Ministry of Education and Research (German Center for Vertigo and Balance Disorders, BMBF, Grant code 01EO140), and the German Hertie Foundation.

Compliance with ethical standards

Conflicts of interest The authors declare they have no conflicts of interest.

References

- Tzourio-Mazoyer N, Seghier ML (2016) The neural bases of hemispheric specialization. *Neuropsychologia* 93:319–324. doi:10.1016/j.neuropsychologia.2016.10.010
- Ocklenburg S, Beste C, Güntürkün O (2013) Handedness: a neurogenetic shift of perspective. *Neurosci Biobehav Rev* 37:2788–2793. doi:10.1016/j.neubiorev.2013.09.014
- Scharoun SM, Bryden PJ (2014) Hand preference, performance abilities, and hand selection in children. *Front Psychol*. doi:10.3389/fpsyg.2014.00082
- Hodgson JC, Hirst RJ, Hudson JM (2016) Hemispheric speech lateralisation in the developing brain is related to motor praxis ability. *Dev Cogn Neurosci* 22:9–17. doi:10.1016/j.dcn.2016.09.005
- Brunetti M, Belardinelli P, Caulo M et al (2005) Human brain activation during passive listening to sounds from different locations: an fMRI and MEG study. *Hum Brain Mapp* 26:251–261. doi:10.1002/hbm.20164
- Coffey EBJ, Herholz SC, Chepesiuk AMP et al (2016) Cortical contributions to the auditory frequency-following response revealed by MEG. *Nat Commun* 7:11070. doi:10.1038/ncomms11070
- Coffey EBJ, Musacchia G, Zatorre RJ (2016) Cortical correlates of the auditory frequency-following and onset responses: EEG and fMRI evidence. *J Neurosci*. doi:10.1523/JNEUROSCI.1265-16.2016
- Dieterich M, Brandt T (2015) The bilateral central vestibular system: its pathways, functions, and disorders. *Ann N Y Acad Sci*. doi:10.1111/nyas.12585
- Dieterich M, Bense S, Lutz S et al (2003) Dominance for vestibular cortical function in the non dominant hemisphere. *Cereb Cortex* 13(9):994–1007
- Fink GR, Marshall JC, Weiss PH et al (2003) Performing allocentric visuospatial judgments with induced distortion of the egocentric reference frame: an fMRI study with clinical implications. *Neuroimage* 20:1505–1517
- Schlindwein P, Mueller M, Bauermann T et al (2008) Cortical representation of saccular vestibular stimulation: VEMPs in fMRI. *Neuroimage* 39:19–31. doi:10.1016/j.neuroimage.2007.08.016
- Janzen J, Schlindwein P, Bense S et al (2008) Neural correlates of hemispheric dominance and ipsilaterality within the vestibular system. *Neuroimage* 42:1508–1518. doi:10.1016/j.neuroimage.2008.06.026
- Zu Eulenburg P, Caspers S, Roski C, Eickhoff SB (2012) Meta-analytical definition and functional connectivity of the human vestibular cortex. *Neuroimage* 60:162–169. doi:10.1016/j.neuroimage.2011.12.032
- Lopez C, Blanke O, Mast FW (2012) The human vestibular cortex revealed by coordinate-based activation likelihood estimation meta-analysis. *Neuroscience* 212:159–179. doi:10.1016/j.neuroscience.2012.03.028
- Guldin WO, Grüsser O-J, Guldin WO, Grüsser OJ et al (1998) Is there a vestibular cortex? *Trends Neurosci* 21:254–259. doi:10.1016/S0166-2236(97)01211-3
- Brandt T, Dieterich M, Danek A (1994) Vestibular cortex lesions affect the perception of verticality. *Ann Neurol* 35:403–412. doi:10.1002/ana.410350406
- Arshad Q, Siddiqui S, Ramachandran S et al (2015) Right hemisphere dominance directly predicts both baseline V1 cortical excitability and the degree of top-down modulation exerted over low-level brain structures. *Neuroscience* 311:484–489. doi:10.1016/j.neuroscience.2015.10.045
- Nigmatullina Y, Siddiqui S, Khan S et al (2016) Lateralisation of the vestibular cortex is more pronounced in left-handers. *Brain Stimul* 9:942–944. doi:10.1016/j.brs.2016.08.001
- Bense S, Bartenstein P, Lutz S et al (2003) Three determinants of vestibular hemispheric dominance during caloric stimulation: a positron emission tomography study. *Ann N Y Acad Sci* 1004:440–445. doi:10.1111/j.1749-6632.2003.tb00256.x
- Kirsch V, Keeser D, Hergenroeder T et al (2016) Structural and functional connectivity mapping of the vestibular circuitry from human brainstem to cortex. *Brain Struct Funct* 221:1291–1308. doi:10.1007/s00429-014-0971-x
- Dieterich M, Brandt T (1993) Thalamic infarctions: differential effects on vestibular function in the roll plane (35 patients). *Neurology* 43:1732–1740
- Baier B, Conrad J, Stephan T et al (2016) Vestibular thalamus two distinct graviceptive pathways. *Neurology* 86:134–140. doi:10.1212/WNL.0000000000002238
- Lopez C, Blanke O (2011) The thalamocortical vestibular system in animals and humans. *Brain Res Rev* 67:119–146. doi:10.1016/j.brainresrev.2010.12.002
- Oldfield RC (1971) The assessment and analysis of handedness: the Edinburgh inventory. *Neuropsychologia* 9:97–113. doi:10.1016/0028-3932(71)90067-4
- Schneider E, Villgratner T, Vockeroth J et al (2009) Eye-SeeCam: an eye movement-driven head camera for the examination of natural visual exploration. *Ann N Y Acad Sci* 1164:461–467. doi:10.1111/j.1749-6632.2009.03858.x
- Dieterich M, Brandt T (1993) Ocular torsion and tilt of subjective visual vertical are sensitive brainstem signs. *Ann Neurol* 33:292–299. doi:10.1002/ana.410330311

27. Behrens TEJ, Woolrich MW, Jenkinson M et al (2003) Characterization and propagation of uncertainty in diffusion-weighted MR imaging. *Magn Reson Med* 50:1077–1088. doi:[10.1002/mrm.10609](https://doi.org/10.1002/mrm.10609)
28. Smith SM (2002) Fast robust automated brain extraction. *Hum Brain Mapp* 17:143–155. doi:[10.1002/hbm.10062](https://doi.org/10.1002/hbm.10062)
29. Behrens TEJ, Berg HJ, Jbabdi S et al (2007) Probabilistic diffusion tractography with multiple fibre orientations: what can we gain? *Neuroimage* 34:144–155. doi:[10.1016/j.neuroimage.2006.09.018](https://doi.org/10.1016/j.neuroimage.2006.09.018)
30. Behrens TEJ, Johansen-Berg H, Woolrich MW et al (2003) Non-invasive mapping of connections between human thalamus and cortex using diffusion imaging. *Nat Neurosci* 6:750–757. doi:[10.1227/01.NEU.0000309595.77090.89](https://doi.org/10.1227/01.NEU.0000309595.77090.89)
31. Putnam MC, Steven MS, Doron KW et al (2010) Cortical projection topography of the human splenium: hemispheric asymmetry and individual differences. *J Cogn Neurosci* 22:1662–1669. doi:[10.1162/jocn.2009.21290](https://doi.org/10.1162/jocn.2009.21290)
32. Dieterich M, Brandt T (2015) The bilateral central vestibular system: its pathways, functions, and disorders. *Ann N Y Acad Sci*. doi:[10.1111/nyas.12585](https://doi.org/10.1111/nyas.12585)
33. Jeffery KJ, Jovalekic A, Verriotis M, Hayman R (2013) Navigating in a three-dimensional world. *Behav Brain Sci* 36:523–543. doi:[10.1017/S0140525X12002476](https://doi.org/10.1017/S0140525X12002476)
34. Jeffery KJ, Wilson JJ, Casali G, Hayman RM (2015) Neural encoding of large-scale three-dimensional space—properties and constraints. *Front Psychol*. doi:[10.3389/fpsyg.2015.00927](https://doi.org/10.3389/fpsyg.2015.00927)
35. Dumont JR, Taube JS (2015) The neural correlates of navigation beyond the hippocampus. *Prog Brain Res* 219:83–102. doi:[10.1016/bs.pbr.2015.03.004](https://doi.org/10.1016/bs.pbr.2015.03.004)
36. Clark BJ, Taube JS (2012) Vestibular and attractor network basis of the head direction cell signal in subcortical circuits. *Front Neural Circuits*. doi:[10.3389/fncir.2012.00007](https://doi.org/10.3389/fncir.2012.00007)
37. Glasauer S, Dieterich M, Brandt T (2017) A modeling approach to explain why unilateral peripheral but not central vestibular lesions manifest with rotational vertigo (**submitted**)
38. Johansen-Berg H, Rushworth MFS (2009) Using diffusion imaging to study human connective anatomy. *Annu Rev Neurosci* 32:75–94. doi:[10.1146/annurev.neuro.051508.135735](https://doi.org/10.1146/annurev.neuro.051508.135735)
39. Jones DK, Knösche TR, Turner R (2013) White matter integrity, fiber count, and other fallacies: the do's and don'ts of diffusion MRI. *Neuroimage* 73:239–254. doi:[10.1016/j.neuroimage.2012.06.081](https://doi.org/10.1016/j.neuroimage.2012.06.081)